*Proc. Natl. Acad. Sci. USA*
Vol. 89, pp. 8376–8380, September 1992
Neurobiology

# Analysis of dynamin isoforms in mammalian brain: Dynamin-1 expression is spatially and temporally regulated during postnatal development

(synaptogenesis/cytoskeleton/microtubule-associated protein/neurogenesis)

KATHLEEN FAIRE*, FRANCINE TRENT†, JAMES M. TEPPER†, AND EDWARD M. BONDER*

*Department of Biological Sciences and †Center for Molecular and Behavioral Neuroscience, Rutgers, The State University of New Jersey, Newark, NJ 07102

*Communicated by Israel M. Gelfand, June 10, 1992 (received for review April 3, 1992)*

ABSTRACT **In adult rat brain, the microtubule-associated protein dynamin is composed of a closely spaced polypeptide doublet of ≈100 kDa. Using an antibody preparation that is monospecific for dynamin-1 (the higher molecular mass isoform) we examined the temporal and regional expression of dynamin-1 in developing rat brain. Analysis of whole rat brain homogenates established that prior to postnatal day 9, dynamin-1 was present only at very low levels and thereafter its expression steadily increased with adult levels being attained by postnatal day 23. In individual regions of the brain, dynamin-1 levels were highest in cortex, amygdala, and striatum, significantly lower in olfactory bulb, cerebellum, and midbrain, and lowest in brainstem. During postnatal development, each of the regions exhibited approximately the same time course of protein expression except for a slight lag in expression in olfactory bulb. The spatial and temporal patterns of expression of dynamin-1 correlate with the establishment and/or maintenance of mature neuronal structure and function rather than dendritic or axonal outgrowth.**

The cytoskeleton of mature neurons is constructed of a complex filamentous assemblage of microtubules, actin microfilaments, and neurofilaments in association with a vast array of accessory proteins. In concert, these proteins serve to generate and maintain the unique morphology of the neuron and to modulate many physiological activities (1–3). Microtubules, the most prominent cytoskeletal component of neuronal processes, are found in association with a heterogeneous group of microtubule-associated proteins (MAPs) and microtubule-dependent motor proteins (1–3). MAPs serve to stabilize microtubule-based structures and/or crosslink these structures to other cytoskeletal elements or cellular organelles (1–3). The mechanoenzyme motor proteins kinesin and dynein possess microtubule-stimulated ATPase activity and evidence suggests they function in anterograde and retrograde axonal transport, respectively (2, 4).

Based on various investigations, it is evident that the interactions of microtubules with MAPs and motor proteins are key regulators of plasticity in developing neuronal processes as well as the stability of mature neuronal processes (for reviews, see refs. 1–3). Although a significant degree of neuronal development occurs prior to birth in mammalian brain, neuronal differentiation, neurite outgrowth, and synapse formation continue postnatally (1–3). During the second and third postnatal week, there is a decrease in axonal and dendritic outgrowth with the accompanying formation of a more stable cytoskeletal organization (1, 3). Coincident with these structural changes is a striking transition in the level of expression or molecular form of numerous brain MAPs (1–3, 5). For example, starting at approximately the second to third postnatal week, the juvenile $\tau$ protein expressed in newborn rat brain is replaced by multiple adult $\tau$ variants (1–3). Presumably, MAPs present early in postnatal development play a role in neuritic extension and the initial establishment of synaptic contacts, whereas adult MAPs function in neuronal process stabilization and the maintenance of mature synapses (1–3, 5).

Recently, Shpetner and Vallee isolated and characterized a 100-kDa polypeptide called dynamin from mammalian brain that demonstrates nucleotide-sensitive binding to microtubules (6) and microtubule-stimulated GTPase (7) activity. Furthermore, under specific conditions, this polypeptide promotes microtubule bundling and intermicrotubule sliding (6). Subsequently, it was found that the predicted amino acid sequence of mammalian brain dynamin (8) shares significant homology with a number of other gene products including shibire from *Drosophila* (9), vps1 (10) and spo15 (11) from yeast, and the Mx proteins from mammalian tissues (12, 13). The homology resides primarily in the amino-terminal half of these molecules and includes a consensus tripartite GTP binding motif (8, 11, 14). Conversely, the carboxyl-terminal halves of these polypeptides are highly divergent, which could provide for functional diversity. As a consequence of the extensive sequence homology surrounding the GTP binding motif, Obar *et al.* (8) suggest that dynamin and these related proteins represent a distinct subgroup within the GTPase protein family. Both interesting and puzzling is the finding that although all of the dynamin-related proteins are structurally similar, none has been demonstrated to interact with microtubules *in vivo*; instead, it has been suggested that they function in different intracellular membrane and vesicle sorting pathways (10–13, 15, 16). Furthermore, even within one dynamin-like family, such as shibire, the existence of several isoforms suggests the potential for functional diversity (14).

Scaife and Margolis (17) isolated dynamin from rat brain and reported its composition as a closely spaced doublet of ≈100 kDa. Given the functional diversity exhibited by the dynamin family of proteins, the existence of different isoforms of dynamin in rat brain raises the possibility that brain dynamin may participate in different cellular functions (11, 14). In this report, we have used antibody probes to demonstrate that the rat brain dynamin doublet is comprised of two immunologically distinct isoforms, dynamin-1 and -2. Furthermore, using monospecific anti-dynamin-1 antibodies, the temporal and regional distribution of this polypeptide was examined in developing and mature brain.

## MATERIALS AND METHODS

**Preparation of Rat Brain Homogenates.** Sprague–Dawley rats, sacrificed by $CO_2$ asphyxiation, were used in the present study. Adult rats were minimally 65 days old with the day of

The publication costs of this article were defrayed in part by page charge payment. This article must therefore be hereby marked "*advertisement*" in accordance with 18 U.S.C. §1734 solely to indicate this fact.

Abbreviations: MAP, microtubule-associated protein; PND, postnatal day(s); NC, nitrocellulose; BSA, bovine serum albumin.

parturition designated as postnatal day (PND) 1. Brains were excised from PND 1, 9, 16, 23, 31 and adult rats and homogenized in PEMG buffer (100 mM Pipes, pH 6.6/1 mM EGTA/1 mM $MgSO_4$/3.4 M glycerol containing 5 mM benzamidine, 2 mM *p*-tosyl-L-arginine methyl ester, 0.15 $\mu$M aprotinin, 1.0 mM phenylmethylsulfonyl fluoride, 0.5 mM dithiothreitol, 100 $\mu$g of soybean trypsin inhibitor per ml) using a ratio of 1.5 ml of buffer per g of wet weight tissue. After homogenization, hot SDS/PAGE sample buffer was added and the preparations were boiled for 5 min. In addition, SDS/PAGE samples were prepared from cortex, amygdala, striatum, cerebellum, olfactory bulb, brainstem, and midbrain of PND 2, 8, 15, 22, 29 and adult rat brains. Five rat brains were dissected for PND 2, four for PND 8, 15, 22, and 29, and two for the adult.

**Polyclonal Antibody Preparation, Immunoblot Analyses, and Blot Affinity Purification.** Anti-sea urchin egg 100-kDa antibody was prepared according to the methods of Granger and Lazarides (18). Samples of brain protein were run on 7.5–15% SDS/polyacrylamide minigels (19, 20) and transferred to nitrocellulose (NC) using the Genie transfer apparatus (Idea Scientific, Minneapolis) at 1 A for 1 hr in 20 mM Tris, pH 8.4/150 mM glycine/12.5% methanol, 0.1% SDS (21). The NC filter was blocked overnight at 4°C in TTBS (50 mM Tris, pH 7.5/150 mM NaCl/0.1% Tween 20/0.02% $NaN_3$) containing 5% fetal calf serum and 1% bovine serum albumin (BSA). The filters were rinsed in TTBS and incubated for 4–5 hr at 25°C with primary antibody (anti-sea urchin egg 100-kDa, affinity-purified anti-dynamin doublet or affinity-purified anti-dynamin-1 antibodies) in TTBS containing 1% BSA followed by five rinses in TTBS. Blots were developed using alkaline phosphatase-conjugated goat anti-rabbit secondary antibody (Cappel Research Products, Durham) according to the methods of Dubreuil *et al.* (22).

Blot affinity-purified anti-brain dynamin-1 antibodies were prepared essentially according to the methods of Olmsted (23). Preparations of rat brain were electrophoresed, transferred to NC, blocked, and probed with a 1:5000 dilution of anti-sea urchin egg 100-kDa immune serum for 24 hr at 25°C. After incubation, the blots were rinsed in TTBS and the appropriate antibody was eluted from the NC with 0.2 M glycine (pH 2.8). The affinity-purified antibody was neutralized with NaOH and diluted into an equal volume of 2× TTBS containing 2% BSA.

Samples of purified calf brain dynamin transferred to NC filters and blot affinity-purified anti-brain dynamin doublet antibody were generously provided by R. Vallee and C. Burgess (Worcester Foundation for Experimental Biology).

**Quantitative Analyses.** To measure the levels of dynamin-1 present in whole brain and brain regions, equivalent amounts of protein were immunoblotted with blot affinity-purified anti-brain dynamin-1 antibody and the results were scanned using an LKB 2400 GelScan XL laser densitometer. Each densitometric scan was integrated a minimum of five times and averaged. The values determined for the developmental time course of dynamin-1 expression in whole rat brain are expressed relative to the level detected in the whole adult brain, whereas those for the expression of dynamin-1 in rat brain regions are relative to the level of dynamin-1 detected in adult cortex. The adult cortex standardization process was achieved by including a lane of adult cortex on each immunoblot experiment and developing each blot to approximately the same intensity. For PND 2 and 8, where the levels of immunoreactivity were low, the immunoblotting and quantification was carried out two or three times and the results were averaged across the trials.

**Other Methods.** Protein concentrations were determined by the method of Bradford (24) using BSA as the standard. SDS/polyacrylamide gels were stained with Coomassie blue according to the procedure of Fairbanks *et al.* (25).

## RESULTS

**Antibody Characterization and Immunological Identification of Rat Brain Dynamin-1.** In a study examining the microtubule cytoskeleton of sea urchin eggs, we isolated a 100-kDa protein that accelerated microtubule polymerization and induced the formation of microtubule bundles (26). Since many MAPs are highly conserved, we used a monospecific polyclonal antibody prepared against the egg 100-kDa protein (Fig. 1*A*, lanes 1 and 2) to investigate the presence of related polypeptides in rat brain. When samples of whole adult rat brains were probed with the anti-egg 100-kDa immune serum there was a highly crossreactive polypeptide at 100 kDa that comigrated with the same molecular mass as the egg protein (Fig. 1*A*). Using the Olmsted procedure of antibody affinity purification (23), the anti-egg 100-kDa immune serum was affinity purified against the brain 100-kDa protein to yield an anti-brain 100-kDa antibody (Fig. 1*A*).

Preliminary studies suggested that the egg 100-kDa protein might be related to the dynamin protein family (26). To determine if the anti-brain 100-kDa antibody bound to dynamin, rat brain preparations were probed with an affinity-purified anti-brain dynamin doublet antibody. The immunoblots demonstrated the presence of a closely spaced immunoreactive dynamin doublet of ≈100 kDa (Fig. 1*A*, lane 6), an observation in agreement with the data of Scaife and Margolis (17). Equivalent dynamin doublets were also observed in calf and hamster brain (K.F. and E.M.B., unpublished data). Comparisons of immunoblots of rat brain using anti-brain 100-kDa and anti-brain dynamin doublet antibodies (Fig. 1*A*, lanes 4 and 6) revealed that the anti-brain 100-kDa antibody was crossreactive with the higher molecular mass polypeptide of the dynamin doublet. Additionally, preparations of purified brain dynamin probed with affinity-purified anti-brain 100-kDa antibody verified that this antibody bound only

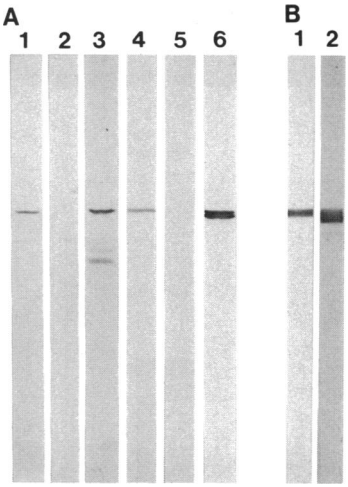


FIG. 1. Identification of rat brain dynamin-1-specific antibody. (*A*) Sea urchin egg total protein immunoblotted with anti-sea urchin egg 100-kDa immune serum (lane 1) and preimmune serum (lane 2). Lanes 3–5, total rat brain protein immunoblotted with anti-sea urchin egg 100-kDa immune serum (lane 3), affinity-purified anti-brain 100-kDa antibody (lane 4), and preimmune serum (lane 5). Note the presence of a single immunoreactive species of 100 kDa in lanes 3 and 4. Total rat brain protein immunoblotted with blot affinity-purified anti-brain dynamin doublet antibody (lane 6) reveals two immunoreactive polypeptides of 100 kDa. (*B*) Purified brain dynamin immunoblotted with affinity-purified anti-brain 100-kDa antibody (lane 1) and affinity-purified anti-brain dynamin doublet antibody (lane 2). In this gel system, the dynamin doublet resolves as a single broad band (lane 2), the upper half of which is recognized by the anti-brain 100-kDa antibody (lane 1).

to the higher molecular mass polypeptide of the rat brain dynamin doublet (Fig. 1*B*, lanes 1 and 2).

For the sake of clarity, we will designate the higher molecular mass polypeptide of the dynamin doublet as dynamin-1 and the lower molecular mass polypeptide as dynamin-2. Consequently, given the specificity of the affinity-purified anti-brain 100-kDa antibody for dynamin-1, this antibody will be referred to as anti-brain dynamin-1 antibody.

**Analysis of Dynamin-1 Expression in Developing Rat Brain.** To examine if dynamin-1 expression is developmentally regulated, preparations of PND 1, 9, 16, 23, 31 and adult rat brain were subjected to immunoblot analysis using the anti-brain dynamin-1 antibody. Whole brains from PND 1 and 9 rat pups, a period characterized by extensive axonal and dendritic outgrowth (2, 3), demonstrated barely detectable levels of dynamin-1 (Fig. 2 *B* and *C*). A major increase in the level of expression occurred between PND 9 and 23 (Fig. 2 *B* and *C*). During this time period the levels of dynamin-1 rose from ≈3% at PND 9 to ≈90% of adult levels by PND 23 (Fig. 2 *B* and *C*). Interestingly, the temporal expression of dynamin-1 correlates with the developmental window marked by diminishing axonal growth and the establishment of mature synaptic contacts (1).

**Regional Expression of Dynamin-1 in Adult Rat Brain.** To determine whether dynamin-1 exhibited regionalized expression, seven morphologically and physiologically distinct areas of the brain (cortex, amygdala, striatum, cerebellum, midbrain, olfactory bulb, and brainstem) were processed for immunoblot analysis and probed with the anti-brain dynamin-1 antibody. There was a marked difference in the level of dynamin-1 expressed in different regions of the adult brain (Fig. 3). Adult cortex, amygdala, and striatum (telencephalon) all exhibited high and relatively equivalent amounts of dynamin-1 (Fig. 3*B*, lanes 1′–3′), whereas the adult brainstem demonstrated the lowest level of dynamin-1 (Fig. 3*B*, lane 6′). Dynamin-1 levels in the other three regions (cerebellum, olfactory bulb, midbrain) were comparable to one another and fell into a range intermediate between the brainstem and telencephalon (Fig. 3*B*, lanes 4′, 5′, and 7′).

**Developmental Analysis of the Regional Expression of Dynamin-1.** Cortex, amygdala, striatum, cerebellum, olfactory bulb, brainstem, and midbrain were removed from PND 2, 8, 15, 22, 29 and adult rat brains and analyzed by quantitative immunoblots. For standardization, each set of PND brain regions and a sample of adult brain cortex were run on single minislab SDS/polyacrylamide gels, transferred to NC, and probed with anti-brain dynamin-1 antibody. By including the adult brain cortex sample within each experimental run it was possible to compare the results of blots that were run with different preparations of tissue and different batches of affinity-purified antibody.

Dynamin-1 was barely detectable in any of the brain regions at PND 2 and 8 (Figs. 4 and 5). With the exception of the olfactory bulb, all of the regions examined showed a similar pattern of expression characterized by a primary rise in the level of dynamin-1 between PND 15 and PND 22 (Fig.

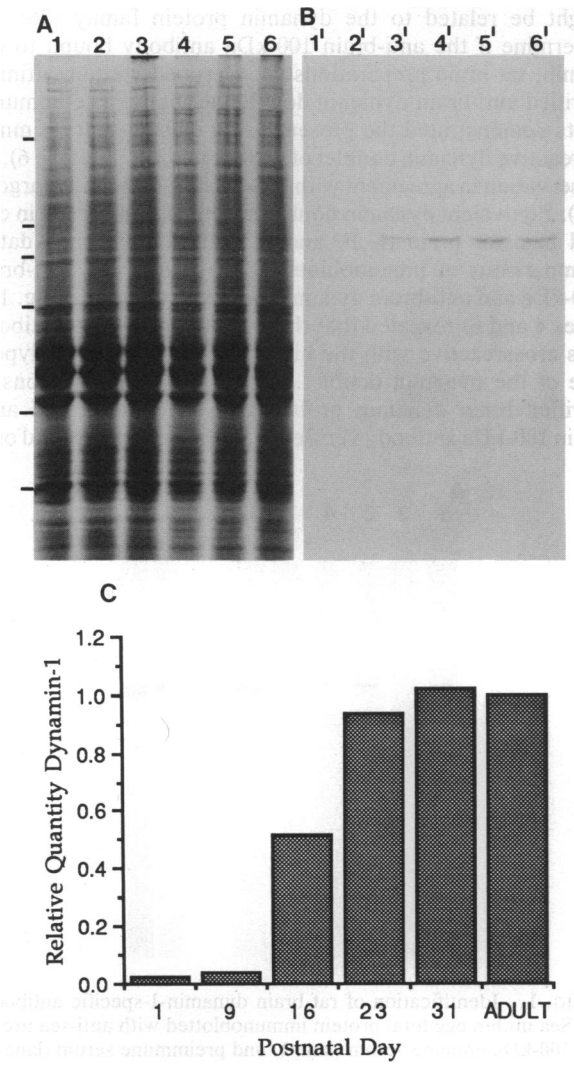


FIG. 2. Analysis of dynamin-1 expression in developing rat brain. (*A*) SDS/PAGE analysis of total protein from developing rat brain. Twenty micrograms of protein from PND 1, 9, 16, 23, 31 and adult rat brains (lanes 1–6, respectively) was separated on 7.5–15% SDS/PAGE. Molecular mass markers are myosin (205 kDa), β-galactosidase (116 kDa), phosphorylase B (97 kDa), BSA (68 kDa), egg albumin (45 kDa), and carbonic anhydrase (29 kDa). (*B*) Developmental expression of rat brain dynamin-1. A companion gel to the one presented in *A* was transferred to NC and immunoblotted with anti-brain dynamin-1 antibody. (*C*) Quantitative analysis of dynamin-1 expression in developing rat brain.

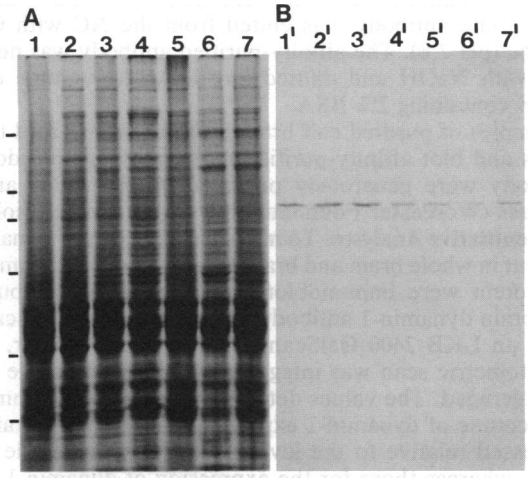


FIG. 3. Regional expression of dynamin-1 in adult rat brain. (*A*) SDS/PAGE analysis of total protein from specific regions of adult rat brain. Twenty-five micrograms of protein from cortex, amygdala, striatum, cerebellum, olfactory bulb, brainstem, and midbrain (lanes 1–7, respectively) of adult rat brains was separated on 7.5–15% SDS/PAGE. Molecular mass markers are myosin (205 kDa), β-galactosidase (116 kDa), phosphorylase B (97 kDa), BSA (68 kDa), egg albumin (45 kDa), and carbonic anhydrase (29 kDa). (*B*) Immunoblot analysis of dynamin-1 in developing rat brain. A companion gel to the one in *A* was transferred to NC and immunoblotted with anti-brain dynamin-1 antibody. Cortex, amygdala, striatum, cerebellum, olfactory bulb, brainstem, and midbrain are shown in lanes 1′–7′, respectively.

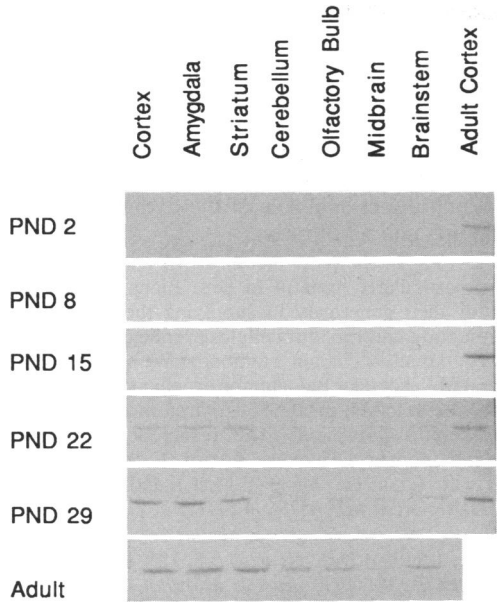


FIG. 4. Immunoblot analysis of the temporal and spatial expression of dynamin-1 in developing rat brain. Samples of total protein were prepared from cortex, amygdala, striatum, cerebellum, olfactory bulb, brainstem, and midbrain of PND 2, 8, 15, 22, 29 and adult rat brains. For each developmental stage and region, an equal amount of protein was separated on 7.5–15% SDS/PAGE, transferred to NC, and immunoblotted with anti-brain dynamin-1 antibody. Only the relevant region of each immunoblot is shown. The brain region is indicated above each lane and the developmental stage is indicated to the left of each individual panel. Expression of dynamin-1 in a particular brain region can be traced throughout postnatal development by following each lane vertically under a designated region. To standardize immunoblots relative to one another, a sample of adult brain cortex was run on each immunoblot.

5). Thus, even though the final level of dynamin-1 differed among these six regions, the developmental pattern of expression was virtually identical. In the olfactory bulb, dynamin-1 expression was slightly delayed with the primary rise in expression occurring between PND 22 and PND 29 (Figs. 4 and 5). This developmental lag was clearly observed when a comparison was made between the relative amount of dynamin-1 in each region of the brain at PND 22 with the amount present in the same region in the adult. Using this comparison, the concentration of dynamin-1 at PND 22 was only 10% of the adult level in olfactory bulb, whereas all other regions exhibited >50% of the adult concentration. In brainstem, adult concentrations of dynamin-1 were reached by PND 22, whereas all other regions attained adult concentrations by approximately PND 29 (Figs. 4 and 5).

## DISCUSSION

The members of the dynamin family of proteins demonstrate a diversity of structure and function (8, 9–13, 15, 16). In the present report, we establish the presence of two immunologically distinct isoforms of dynamin in mammalian brain, dynamin-1 and -2. By immunoblot analyses, dynamin-1 was found to be developmentally regulated during postnatal maturation of the rat brain. In adult brain, dynamin-1 was most abundant in telencephalon (cortex, amygdala, striatum) and least abundant in brainstem. Intermediate levels were observed for cerebellum, olfactory bulb, and midbrain. Dynamin-1 expression in each of the regions followed approximately the same developmental pattern with the principal increase in expression occurring between PND 15 and 22, except for delayed expression in the olfactory bulb.

An understanding of the functional diversity present within the dynamin protein family is essential when considering the potential function(s) of mammalian brain dynamin-1 and -2. To date, molecular genetic analysis in *Drosophila*, yeast, and mice presents a very compelling argument for participation of the dynamin protein family in membrane and vesicle sorting (9–16), processes of crucial importance for synaptic function in the nervous system. The shibire locus in *Drosophila* encodes several dynamin-like polypeptides, one of which (Ddyn4) has a predicted amino acid sequence 68% identical to rat brain dynamin (14). One or all of the shibire products may be linked to synaptic vesicle recycling at neuromuscular junctions, and mutations in the shibire locus result in flies that exhibit temperature-sensitive paralysis (9, 14–16). Further, yeast vps1 and mammalian Mx1, both dynamin-like proteins, are thought to function in intracellular vesicle sorting (10, 12, 13). Interestingly, the yeast *SPO15* locus, which is identical to *VPS1*, has not been implicated in vesicle sorting but instead functions in centrosome separation during meiotic division (11). Thus, although all of the dynamin-like proteins appear highly conserved in the amino-terminal half of the individual molecules, they appear to participate in a number of different functions presumably determined by the structural diversity of the carboxyl-terminal half of the protein (7, 8).

Nakata *et al.* (27) examined the expression of rat brain dynamin and reported increases in the level of expression between PND 7 and 15 and dynamin mRNA localization was highest in neurons. However, that study did not differentiate between brain dynamin isoforms. Our data complement and extend their results by specifically examining the spatial and temporal expression of the dynamin-1 isoform. Developmental expression of dynamin-1 correlates with the expression of other adult neuronal MAPs that appear to function in neuronal process stabilization. For example, MAP2a, which serves to stabilize the adult microtubule cytoskeleton, first

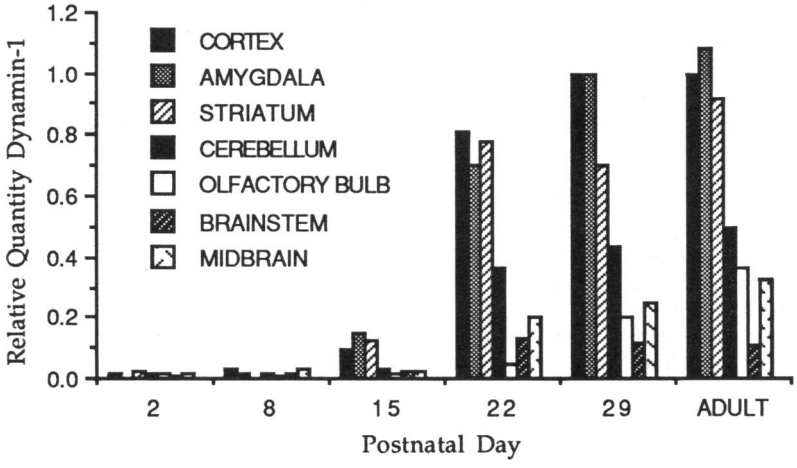


FIG. 5. Quantitative analysis of the spatial and temporal expression of dynamin-1. Rat brain regions were immunoblotted using anti-brain dynamin-1 antibodies and the resultant immunoblots were scanned using an LKB laser densitometer. The level of dynamin-1 detected in each region at each developmental stage was quantified relative to the level of dynamin-1 immunoreactive product in the adult cortex (see Fig. 4).

appears around PND 10 and continues to increase until PND 20 when adult levels are reached, whereas MAP2c expression, which correlates with axon formation, decreases dramatically between PND 10 and 20 (2, 3, 5). Further, since the majority of neurons in rat brain have already undergone significant axonal and dendritic extension by PND 22, the dramatic increase in dynamin-1 expression that occurs between PND 15 and 22 indicates that it is highly unlikely that dynamin-1 plays a role in dendritic or axonal outgrowth. However, dynamin-1 could serve to stabilize the microtubule cytoskeleton of mature neurons. In support of this potential role are the observations that yeast spo15 (11), sea urchin egg (26), calf (6), and rat brain (8) dynamins all bind to microtubules *in vitro*. Though this hypothesis is appealing, it does not explain the low levels of dynamin-1 expression in regions of the brain that are rich in axonal fibers, such as brainstem, and the apparent lack of any obvious dynamin/microtubule colocalization in differentiated PC12 cells (17).

Could dynamin-1 participate in a neuronal function other than the organization of the microtubule cytoskeleton? We observed the highest levels of dynamin-1 expression in the telencephalon, a region characterized by a highly dense and complex synaptic neuropil, whereas the lowest levels were found in brainstem, a region that contains a large number of fibers passing from the forebrain to the spinal cord without making synaptic contacts. Further, dynamin-1 levels increase dramatically between PND 15 and 22, the approximate time frame during which the cortical and thalamic afferents to neostriatum form the bulk of their synaptic contacts (28). Likewise, the increase in dynamin-1 levels in midbrain correlates with the timing of synaptic and physiological maturation in this brain region (29). Conversely, the expression of dynamin-1 remains low in the adult olfactory bulb, a region where juvenile MAPs are known to persist in the adult and where neurite extension and the formation of new synapses continue in the adult (30).

In addition to the above correlations between synapse formation and dynamin-1 expression, it is interesting to note that the temporal course of dynamin-1 expression follows the same pattern as the mature synaptic terminal proteins synaptophysin and NT75 (31). The nerve terminal protein NT75 is expressed in cerebellum beginning at PND 7 and maximal levels are reached between PND 20 and 30 (31). Likewise, levels of synaptophysin in the cerebellum increase dramatically during the first 3 postnatal weeks of development (31). Thus, the temporal pattern of expression of dynamin-1 virtually mirrors that of NT75 and synaptophysin. Additionally, previous studies on rat brain development found high levels of expression of growth-associated protein 43 (GAP-43), a phosphoprotein localized to nerve terminals, during neurite outgrowth and a rapid decrease coincident with the formation of mature synaptic contacts (32). Specifically, levels of GAP-43 in the cortex are high at birth and steadily decline following PND 8. In cortex, dynamin-1 expression follows precisely the opposite pattern, with barely detectable levels of expression prior to PND 8, thereafter increasing until PND 20 when adult levels are reached (Fig. 5). Thus, dynamin-1 expression appears to be correlated with the development of mature synaptic contacts in postnatal rat brain development, and this finding is consistent with the potential role of the shibire locus in *Drosophila*.

The potential participation of dynamin-1 in synaptic maturation and vesicle recycling has significant impact on our understanding of postnatal brain development. However, numerous synaptic contacts have been established prior to birth in the rat brain and there is likely ongoing synaptic vesicle membrane recycling. Likewise, membrane recycling occurs during neurite extension. In the absence of significant levels of dynamin-1 in brains of newborn rats, dynamin-2 or other as yet unidentified dynamin-like molecules could participate in membrane recycling and synaptic function in newborn brain. Future immunocytochemical studies, aimed toward defining the cellular localization of the dynamin isoforms during development, should provide insight into the potential multifunctional role of the dynamin protein family in developing and adult brain.

We are particularly grateful to Drs. Richard Vallee and Chris Burgess for their generosity in supplying the anti-brain dynamin doublet antibody and the nitrocellulose replicas used in the characterization of our anti-dynamin-1 antibody. We also thank Mr. Robert Harrell and Ms. Adenike Balogun for excellent technical assistance. Special thanks go to Ms. Lisanne D'Andrea and Mr. Fengsong Wang for many helpful discussions. This research was supported by a Johnson and Johnson Discovery Award (E.M.B.), National Institutes of Health Grant HD 24649 (E.M.B.), and National Institute of Mental Health Grant MH 45286 (J.M.T.).

1. Nunez, J. (1986) *Dev. Neurosci.* **8**, 125–141.
2. Riederer, B. M. (1990) *Eur. J. Morphol.* **28**, 347–378.
3. Tucker, R. P. (1990) *Brain Res. Rev.* **15**, 101–120.
4. Schroer, T. A. & Sheetz, M. P. (1991) *Annu. Rev. Physiol.* **53**, 629–652.
5. Riederer, B. & Matus, A. (1985) *Proc. Natl. Acad. Sci. USA* **82**, 6006–6009.
6. Shpetner, H. S. & Vallee, R. B. (1989) *Cell* **59**, 421–432.
7. Shpetner, H. S. & Vallee, R. B. (1992) *Nature (London)* **355**, 733–735.
8. Obar, R. A., Collins, C. A., Hammarback, J. A., Shpetner, H. S. & Vallee, R. B. (1990) *Nature (London)* **347**, 256–261.
9. van der Bliek, A. M. & Meyerowitz, E. M. (1991) *Nature (London)* **351**, 411–414.
10. Rothman, J. H., Raymond, C. K., Gilbert, T., O'Hara, P. J. & Stevens, T. H. (1990) *Cell* **61**, 1063–1074.
11. Yeh, E., Driscoll, R., Coltrera, M., Olins, A. & Bloom, K. (1991) *Nature (London)* **349**, 713–715.
12. Arnheiter, H. & Meier, E. (1990) *New Biologist* **2**, 851–857.
13. Arnheiter, H., Skuntz, S., Noteborn, M., Chang, S. & Meier, E. (1990) *Cell* **62**, 51–61.
14. Chen, M. S., Obar, R. A., Schroeder, C. C., Austin, T. W., Poodry, C. A., Wadsworth, S. C. & Vallee, R. B. (1991) *Nature (London)* **351**, 583–586.
15. Poodry, C. A. & Edgar, L. (1979) *J. Cell Biol.* **81**, 520–527.
16. Kosaka, T. & Ikeda, K. (1983) *J. Cell Biol.* **97**, 499–507.
17. Scaife, R. & Margolis, R. L. (1990) *J. Cell Biol.* **111**, 3023–3033.
18. Granger, B. L. & Lazarides, E. (1979) *Cell* **18**, 1053–1063.
19. Laemmli, U. K. (1970) *Nature (London)* **227**, 680–685.
20. Matsudaira, P. T. & Burgess, D. R. (1978) *Anal. Biochem.* **87**, 386–396.
21. Towbin, H., Staehelin, T. & Gordon, J. (1979) *Proc. Natl. Acad. Sci. USA* **76**, 4350–4354.
22. Dubreuil, R., Byers, T. J., Branton, D., Goldstein, L. S. B. & Kiehart, D. P. (1987) *J. Cell Biol.* **105**, 2095–2102.
23. Olmsted, J. B. (1981) *J. Biol. Chem.* **256**, 11955–11957.
24. Bradford, M. M. (1976) *Anal. Biochem.* **72**, 248–254.
25. Fairbanks, G., Steck, T. L. & Wallach, D. F. H. (1971) *Biochemistry* **10**, 2606–2617.
26. Faire, K. & Bonder, E. M. (1991) *J. Cell Biol.* **115**, 35a (abstr.).
27. Nakata, T., Iwamoto, A., Noda, Y., Takemura, R., Yoshikura, H. & Hirokawa, N. (1991) *Neuron* **7**, 461–469.
28. Hattori, T. & McGeer, P. L. (1973) *Exp. Neurol.* **38**, 70–79.
29. Tepper, J. M., Trent, F. & Nakamura, S. (1990) *Dev. Brain Res.* **54**, 21–33.
30. Viereck, C., Tucker, R. P. & Matus, A. (1989) *J. Neurosci.* **9**, 3547–3557.
31. Wright, D. J., Ritchie, T. C. & Coulter, J. D. (1991) *J. Compar. Neurol.* **304**, 530–543.
32. Dani, J. W., Armstrong, D. M. & Benowitz, L. I. (1991) *Neuroscience* **40**, 277–287.